ment of Diameter-Pressure Relationship in Carotid Arteries from Normotensive and Spontaneously Hypertensive Rats,'' J. Hypertens. Suppl., **10**(6), p. S27–30.
[29] Stefanadis, C., Dernellis, J., Tsiamis, E., Diamantopoulos, L., Michaelides, A., and Toutouzas, P., 2000, ''Assessment of Aortic Line of Elasticity Using Polynomial Regression Analysis,'' Circulation, **101**(15), p. 1819–25.
[30] Hayashi, K., Handa, H., Nagasawa, S., Okumura, A., and Moritake, K., 1980, ''Stiffness and Elastic Behavior of Human Intracranial and Extracranial Arteries,'' J. Biomech., **13**(2), p. 175–84.
[31] Bank, A. J., Wang, H., Holte, J. E., Mullen, K., Shammas, R., and Kubo, S. H., 1996, ''Contribution of Collagen, Elastin, and Smooth Muscle to in Vivo Human Brachial Artery Wall Stress and Elastic Modulus,'' Circulation, **94**(12), p. 3263–70.
[32] Zulliger, M. A., Montorzi, G., and Stergiopulos, N., 2002, ''Biomechanical Adaptation of Porcine Carotid Vascular Smooth Muscle to Hypo and Hypertension in Vitro,'' J. Biomech., **35**(6), p. 757–65.
[33] Hayashi, K., Takamizawa, K., Nakamura, T., Kato, T., and Tsushima, N., 1987, ''Effects of Elastase on the Stiffness and Elastic Properties of Arterial Walls in Cholesterol-Fed Rabbits,'' Atherosclerosis, **66**(3), p. 259–67.
[34] Faury, G., Maher, G. M., Li, D. Y., Keating, M. T., Mecham, R. P., and Boyle, W. A., 1999, ''Relation between Outer and Luminal Diameter in Cannulated Arteries,'' Am. J. Physiol., **277**(5 Pt 2), p. H1745–53.

Feasibility of Using Orthogonal Fluoroscopic Images to Measure In Vivo Joint Kinematics

Guoan Li,[1] Thomas H. Wuerz,[1] and Louis E. DeFrate[1,2]
[1]Bioengineering Laboratory, Department of Orthopaedic Surgery, Massachusetts General Hospital and Harvard Medical School, Boston, MA
[2]Department of Mechanical Engineering, Massachusetts Institute of Technology, Cambridge, MA

Accurately determining in vivo knee kinematics is still a challenge in biomedical engineering. This paper presents an imaging technique using two orthogonal images to measure 6 degree-of-freedom (DOF) knee kinematics during weight-bearing flexion. Using this technique, orthogonal images of the knee were captured using a 3-D fluoroscope at different flexion angles during weight-bearing flexion. The two orthogonal images uniquely characterized the knee position at the specific flexion angle. A virtual fluoroscope was then created in solid modeling software and was used to reproduce the relative positions of the orthogonal images and X-ray sources of the 3-D fluoroscope during the actual imaging procedure. Two virtual cameras in the software were used to represent the X-ray sources. The 3-D computer model of the knee was then introduced into the virtual fluoroscope and was projected onto the orthogonal images by the two virtual cameras. By matching the projections of the knee model to the orthogonal images of the knee obtained during weight-bearing flexion, the knee kinematics in 6 DOF were determined. Using regularly shaped objects with known positions and orientations, this technique was shown to have an accuracy of 0.1 mm and 0.1 deg in determining the positions and orientations of the objects, respectively. [DOI: 10.1115/1.1691448]

Corresponding author: Bioengineering Laboratory, 55 Fruit Street, GRJ 1215, Boston, MA 02114. Phone: (617)-726-6472; Fax: (617)-724-4392; e-mail: gli1@partners. orq.

Contributed by the Bioengineering Division for publication in the JOURNAL OF BIOMECHANICAL ENGINEERING. Manuscript received by the Bioengineering Division, June 3, 2003; revision received October 27, 2003. Associate Editor: K. Vaugh.

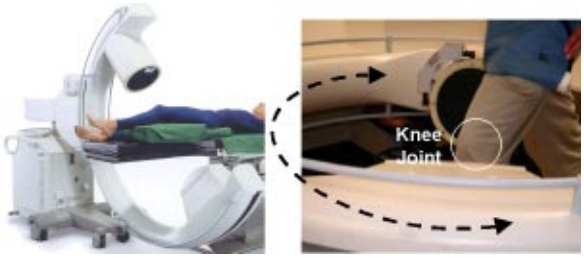

Fig. 1 The 3-D fluoroscopy system: (*a*) 3-D scanning of the knee; and (*b*) acquisition of 2-D images with the knee positioned inside the C-arm.

Introduction

Accurately measuring in vivo knee kinematics remains a technically difficult topic in biomedical engineering. Most gait laboratories measure joint kinematics by using multiple video cameras [1,2]. Due to the relative motion between the skin and the underlying bones, there is a certain degree of inaccuracy inherent to this technique. To improve the accuracy of kinematics measurements, reflective markers have been directly fixed to bone using thin rods [3]. Roentgen opaque markers have also been imbedded within the bones and used to measure knee motion using dual X-ray images [4–7]. In order to improve accuracy without using invasive measurement techniques, a point cluster technique has been proposed to reduce the effect of relative skin and bony motions [8].

Recently, 2-D fluoroscopy has been used to measure in vivo total knee arthroplasty kinematics because of its simplicity and accessibility [9,10]. In these studies, a single, sagittal plane image of the knee was taken at different flexion angles. The positions of 3-D computer models of the prosthesis were manipulated so that their projections on the image plane matched those captured during in vivo knee motion. The relative positions of the 3-D components therefore represented the in vivo knee kinematics. While the single fluoroscopic image technique has been shown to have good accuracy in determining knee position along the axes parallel to the image plane, its accuracy in determining knee motion in the direction perpendicular to the image plane has been questioned [11,12]. The ability of this technique to accurately measure in vivo knee kinematics in six degrees of freedom (6 DOF) has yet to be proved.

In this paper, we present a technique using two orthogonal images of the knee to measure 6 DOF knee kinematics using a 3-D fluoroscope. The knee position was determined by matching the projections of a 3-D knee model to the images of the knee on the two orthogonal images. This study assessed the accuracy of the technique in measuring the relative position and orientation of two 3-D objects and used the technique to measure the 6 DOF kinematics of the knee joint during weight-bearing flexion.

Materials and Methods

3-D Fluoroscope. A 3-D fluoroscope (SIREMOBIL Iso-C^{3D}, Siemens, Germany) was used to capture images of the knee joint in this study (Fig. 1). In order to construct a 3-D knee model, the C-arm of the fluoroscope was positioned vertically. The C-arm rotated about the knee joint through a range of 190 deg and captured 100 images using a pulsed imaging sequence to create an isotropic image database of the joint (Fig. 1(*a*)). Total scan time was approximately 80s. This database allowed the knee to be viewed and sliced from an arbitrary angle to create a series of

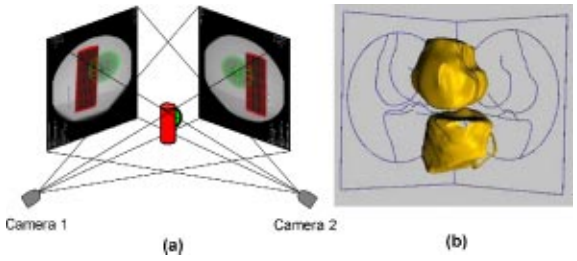

Fig. 2 (*a*) Reproduction of the relative position of the ball and cylinder using two orthogonal images taken from the 3-D fluoroscope; (*b*) Determination of knee positions using 3-D knee models and orthogonal images of the knee from anteromedial and posteromedial views.

images in DICOM file format. These images were exported to a solid modeling software and used to create 3-D computer models of the knee [13].

In order to generate conventional 2-D x-rays of the knee at different flexion angles during in vivo knee flexion, the C-arm of the 3-D fluoroscope was positioned in the horizontal plane (Fig. 1(*b*)). The x-ray images could be taken at any specific view angle around the joint. In the current study, this function of the fluoroscope was used to generate images of the knee from two orthogonal directions (anteromedial and anterolateral).

The distance between the X-ray source and the image intensifier of the fluoroscope is 988 mm. The size of the acquired 3-D data cube is approximately 128 mm×128 mm×128 mm. The resolution is approximately equal to a voxel size of 0.4 mm. The amount of radiation exposure from the 3-D fluoroscope is 30 times lower than that from a standard CT scan. During the protocol used in this study, a subject is exposed to an effective dose of much less than 50 millirems.

Validation of Dual Orthogonal Imaging Technique to Measure Position of 3-D Objects. Our use of a dual orthogonal imaging technique to investigate the relative position and orientation of 3-D objects was validated by scanning a ball-cylinder combination with known relative positions. The ball had a diameter of 47.6 mm. The cylinder had a diameter of 31.75 mm and length of 88.9 mm. The long axis of the cylinder was positioned perpendicularly to the ground and the ball was positioned so that it was in contact with the side of the cylinder. The shortest distance between the center of the ball and the surface of the cylinder was the radius of the ball (23.8 mm). The ball and cylinder were placed in the center of the C-arm of the 3-D fluoroscope (called the isocenter). Four laser beams fixed on the C-arm were used to determine the position of the isocenter in space. The distance from the X-ray source to the isocenter is 622 mm and from the isocenter to the image intensifier of the fluoroscope is 366 mm. Two orthogonal images of the ball-cylinder combination were taken with the C-arm in the horizontal plane, representing the ball-cylinder combination viewed from the two orthogonal directions. The outlines of the objects were specified from both images.

The ball and cylinder positions were reproduced in a solid modeling software (Rhinoceros®, Robert McNeel & Associates, Seattle, WA) using the two orthogonal images and 3-D models of the ball and cylinder. First, the two X-ray images of the ball and cylinder were imported into the software and placed in two orthogonal planes. Next, two ''virtual C-arms'' were created by placing two cameras within the software at an exact distance from the plane of the image, based on the geometry of the C-arm. These two cameras enabled 3-D objects created within the software to be viewed from the two orthogonal directions corresponding to the position of the C-arm during imaging. The positions and orientations of the 3-D models of the ball and cylinder were manually manipulated within the software, so that their projections matched the two orthogonal fluoroscopic images. Each virtual camera projected the objects onto the corresponding image plane (Fig. 2(*a*)). The software allowed for the adjustment of the positions of the ball and cylinder models in 6 DOF, including translations along and rotations about the three axes of the coordinate system of the virtual space.

After positioning the objects, the two virtual cameras projected the objects onto the orthogonal images and represented the perspective views of the ball-cylinder combination as generated by the C-arm. Using the two orthogonal images, translation in the direction perpendicular to one image represented the in-plane motion of another image. Therefore, the 6 DOF position of an object can be accurately determined using the orthogonal images, overcoming the limitations of using a single sagittal plane image.

The distance from the center of the ball to the surface of the cylinder and the orientation of the cylinder were determined for five independent trials by one investigator. These results were compared to the known data in order to investigate the accuracy of this technique in reproducing the relative position of the ball and cylinder, and orientation of the cylinder. In order to compare the current method with a method using a single sagittal plane image, only one image was used to define the spatial position of the ball. The ball model was then moved along the axis perpendicular to the single image plane, and the change in diameter of its projection on the image plane and the change of its projection position on the orthogonal image plane were measured.

Application to the Measurement of In Vivo Knee Joint Kinematics

In order to demonstrate the ability of this technique to measure in vivo joint kinematics, we determined in vivo knee kinematics during knee flexion under weight-bearing conditions in three knees (one left knee from a female and two right knees from males, with an average age of 26 years old) using a protocol approved by the IRB at Massachusetts General Hospital. A 3-D computer knee model was constructed for each knee using the images of the knee scanned by the 3-D fluoroscope. One hundred projections of the knee were taken as the fluoroscope rotated about the joint. Parallel images were generated from the database created by the 3-D fluoroscope and imported into the Rhinoceros software. The outlines of the bones were digitized and used to construct a solid knee model [13]. This model included the bony geometry of both the tibia and femur (Fig. 2(*a*)).

Sets of two orthogonal images were taken during weight-bearing knee flexion at 0, 30, 60, 90 and 120 deg of flexion (Fig. 1(*b*)). Subjects stood upright on a platform and the C-arm was positioned in the horizontal plane. In order to allow for the positioning of the subjects near the isocenter without obstructing image acquisition, subjects spread their legs apart in the anteroposterior direction. Acquiring the two orthogonal images at each flexion angle took less than 4 seconds. The two images for each flexion angle were from the posterolateral and anterolateral views for right knees, posteromedial and anteromedial views for left knees.

The 3-D knee model and its corresponding dual orthogonal images were imported into the virtual C-arm. The positions of the tibial and femoral models were manually adjusted in 6 DOF until the projected outlines of the knee model matched the orthogonal images obtained from the fluoroscope (Fig. 2(*b*)). This procedure was similar to the techniques used by others [14]. The knee kinematics were then determined using the knee models at each flexion angle. In this study, the knee position at full extension position was used as a reference. We measured the tibiofemoral contact points on the medial and lateral tibial plateau as well as the internal-external tibial rotation during weight-bearing flexion of the knee. Tibiofemoral contact points were defined as the location where the distances between the femoral condyle and the tibial

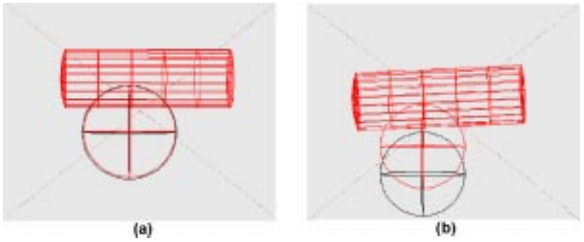

Fig. 3 This figure shows the effects of slightly mismatching the diameter of the ball in one plane on the position of the ball in the orthogonal plane. A slight mismatch of the position of the ball in plane (*a*) results in a large error in the position of the ball in the orthogonal plane (*b*).

plateau were the shortest. The contact points were measured positive anterior to and negative posterior to the midline of the tibial plateau. The midline was defined as the line connecting the center points between the anterior and posterior edges of the medial and lateral plateau of the tibia. Tibial rotation was defined as the rotation around the longitudinal axis of the tibia during flexion [15].

Results

Accuracy of the Orthogonal Image Technique. The models of the ball and the cylinder were adjusted in the virtual C-arm of the 3-D fluoroscope (Fig. 2(*a*)). Their projections on the orthogonal images were compared to the image outlines of the objects obtained in the real fluoroscopic scan experiment (Fig. 3). The average error for the five trials in measuring the distance between the center of the ball and the surface of the cylinder was within 0.1 mm compared to the known distance value. The orientation of the cylinder was determined to have an average accuracy within 0.1 deg.

The sensitivity of using a single image matching technique to determine the ball position was also investigated, as shown in Fig. 4. When the ball was initially positioned at the central position between the camera and the image intensifier, moving the ball towards and away from the camera by 10 mm caused the diameter of the projection of the ball to increase and decrease by 0.5 mm in the image plane. When the object was positioned closer to the image intensifier (100 mm), moving the object towards and away from the camera by 10 mm caused the diameter of the projection to increase and decrease by 0.25 mm.

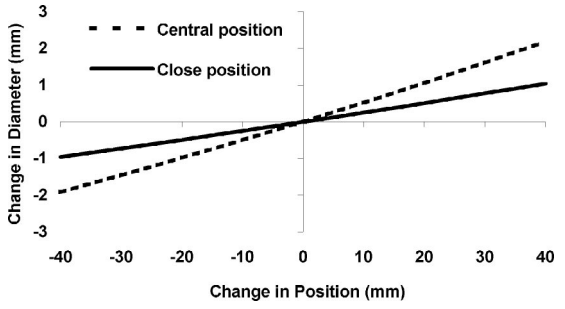

Fig. 4 The change in diameter of the ball's projection on the image intensifier as the ball's position is changed in perpendicular direction ("−" moving towards and "+" moving away from the orthogonal image intensifier). The center position refers to varying the position of the ball relative to a position located at the isocenter of the fluoroscope, and the close position refers to a position 100 mm closer to the image intensifier.

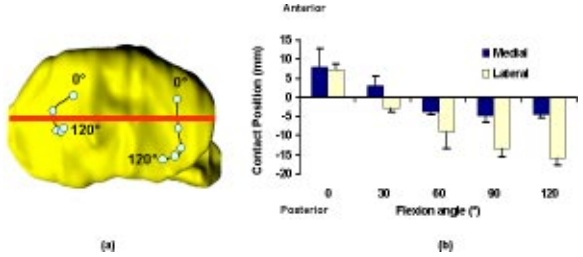

Fig. 5 (*a*) Tibiofemoral contact points at different flexion angles during in-vivo weight-bearing lunge of a typical subject; (*b*) Tibiofemoral contact points of the three subjects versus flexion angle during in-vivo weight bearing lunge (mean ± standard deviation). Positive values are anterior to the midline of the medial/lateral tibial plateaus and negative values are posterior to the midline.

In Vivo Weight-Bearing Knee Kinematics. The tibiofemoral contact points on the tibial plateau as a function of flexion for a typical subject are shown in Fig. 5(*a*). Figure 5(*b*) depicts the mean and standard deviation of the positions of the contact points on the tibial plateau as a function of flexion for the three specimens. At full extension, the contact points in both the medial and lateral compartments were anterior to the midline of the knee at full extension (Fig. 5). The medial contact point was anterior to the midline by 7.9 ± 5.1 mm (mean ± standard deviation) and the lateral contact points by 7.3 ± 1.5 mm. The contact points shifted posteriorly at 30 deg (2.9 ± 2.6 mm and −2.8 ± 1.0 mm for the medial and lateral, respectively) and 60 deg of flexion (−3.9 ± 0.6 mm and −9.1 ± 4.3 mm, respectively). Beyond 60 deg of flexion, the medial contact points remained at the same location with increasing flexion. However, the lateral tibiofemoral contact consistently moved posteriorly with increasing flexion. At 120 deg, the lateral tibiofemoral contact moved to −16.0 ± 1.6 mm. The contact point shifted to the posterior-medial position of the lateral tibial plateau; the lateral femoral condyles moved toward the posterior edge of the tibial plateau (Fig. 5(*a*)).

The axial tibial rotation of the subjects during in vivo weight-bearing flexion is shown in Fig. 6. The internal tibial rotation increased sharply to 12.6 ± 4.3 deg at 30 deg of flexion. Thereafter, tibial rotation slightly increased to 15.2 ± 2.5 deg at 60 deg of flexion. The tibial rotation consistently increased after 60 deg of flexion and reached 25.8 ± 3.7 at 120 deg of flexion.

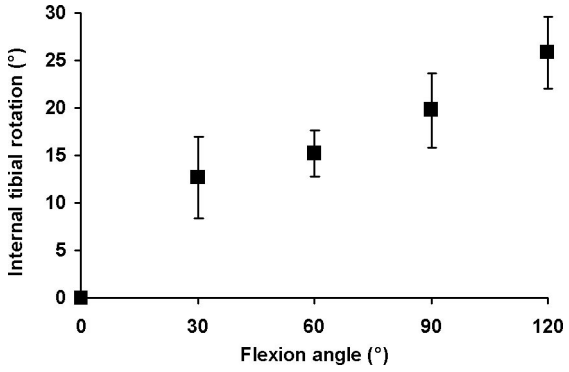

Fig. 6 Internal tibial rotation of the three subjects versus flexion angle during in-vivo weight bearing lunge (mean ± standard deviation)

Discussion

Using a single 2-D projectional fluoroscopic image to investigate knee kinematics is a recent development in in vivo biomechanics research [9,16]. In this approach, a 3-D knee model is manipulated until its projection matches the geometry of the 2-D image [9,12]. The accuracy of determining knee position in the plane of the 2-D fluoroscopic image has been reported in the literature [11,12]. However, this method may not be ideal for the determination of joint position in the direction perpendicular to plane of the image.

The current study measured the change in diameter of the projection of a ball on a single image when varying the position of the ball along the line perpendicular to the image plane. These data demonstrated that a small error in matching an object to its 2-D flouroscopic image could cause a large variation in its position in the perpendicular direction of the image. Figure 3 shows that a slight mismatch in the diameter of the ball in one image plane (0.2 mm in Fig. 3(*a*)) caused a much larger translation error in the other orthogonal plane image (8 mm in Fig. 3(*b*)). Therefore, only matching a single planar image to a 3-D knee model may be insufficient to determine 6 DOF joint motion. A recent study using a single sagittal plane image technique [12] assumed that the knee is constrained in medial-lateral direction and neglected the displacement in the medial-lateral direction.

To overcome the disadvantage of the one image technique, this paper used two orthogonal fluoroscopic images to determine 6 DOF knee joint kinematics. With two orthogonal images, the translation of the object in the direction perpendicular to one image is the in-plane motion of the other image. As shown in Fig. 3, the small mismatch in one plane (Fig. 3(*a*)) is enlarged approximately 15 times in the orthogonal plane (Fig. 3(*b*)). In the two image technique, this error would be much more apparent. Thus the position of the object in space can be more accurately determined using the two orthogonal images. The accuracy of the two orthogonal image technique was shown to be 0.1 mm in translation and 0.1 deg in orientation using the ball-cylinder combination.

The feasibility of using the 3-D fluoroscopic technique to study in vivo human knee kinematics was assessed during a weight-bearing lunge in three human subjects. The knee models were constructed using the images generated from the 3-D fluoroscope. In all of the knees, internal tibial rotation increased with flexion, which is consistent with previous studies in the literature [12,14,17]. The tibiofemoral contact points were shown to move posteriorly at low flexion angles. Beyond 60 deg, the medial tibiofemoral contact locations did not translate posteriorly, but the lateral contact locations continued to move posteriorly. These data are also consistent with previous reports in the literature [12,17]. However, our data also demonstrates that the contact points translate in the medial and lateral direction. For example, the lateral contact locations were observed to move medially on the tibial plateau at high flexion angles. An accurate description of knee kinematics is especially important when accurate kinematics data is needed to determine cartilage contact area and ligamentous tension during in vivo knee joint activities.

Previous studies have used conventional X-ray images to investigate knee kinematics [11,14]. In these studies, a CT scan of the knee was used to represent the geometry of the native knee. You et al. [11] matched the bony density pattern of each of the two X-ray images individually using the projections of the CT image models of the knee. The final orientations of the knee were calculated as the average of the data obtained from the two individual images. Asano et al. [14] matched a CT knee model to the X-ray images of the knee in the anteroposterior view and the mediolateral view to calculate knee joint rotation, similar to the technique used in current study. However, obtaining anterior view X-ray images may be technically difficult as the knee flexion angle increases.

Compared with these methods, the current study used a low dosage 3-D fluoroscope to acquire an image set of the knee to create an anatomic knee model. The orthogonal images were taken with the knee joint positioned in the isocenter of the fluoroscope as the C-arm rotates around the joint in the horizontal plane. The knee was imaged from the anteromedial and anterolateral directions. The overall imaging procedure for scanning one subject took less than 30 minutes. This includes the 80 s required for the 3-D scan of the knee and the resting time between weight-bearing flexion angles. Acquiring the two orthogonal images at each flexion angle during weight-bearing flexion only required about 4 s, which makes this technique a useful tool for measuring in vivo joint kinematics.

There are several limitations to the current study, which may need to be addressed in the future. The weight-bearing lunge was scanned statically at each flexion angle in the current study and did not measure dynamic motion of the joint. During the test, the subject had to maintain their position for the four seconds required for imaging. However, none of the subjects had difficulty maintaining a stationary position during the test. Also, the 3-D knee models were constructed using the images captured by the 3-D fluoroscope. The geometry of the cartilage and meniscus could not be measured by using the 3-D fluoroscope to generate the knee models. Furthermore, the contact points were determined by finding the locations where the distances between the femur and the tibia are the shortest. In the future, an MR image based knee model will be used to investigate ligament elongation and cartilage contact patterns. Despite these limitations, the orthogonal image technique using the 3-D fluoroscope presents a useful methodology for the determination of quasi-static joint kinematics in 6 DOFs. The entire imaging procedure was completed within 30 minutes, making it possible to evaluate patients with knee injuries. This technique is readily applicable to the biomechanical study of all other joints such as the wrist, elbow, shoulder, foot and ankle.

Acknowledgment

The technical support of Richard Johnson was greatly appreciated. Siemens provided the 3-D fluoroscope.

References

[1] Georgoulis, A. D., et al., 2003. Three-dimensional tibiofemoral kinematics of the anterior cruciate ligament-deficient and reconstructed knee during walking. Am. J. Sports Med., **31**(1), pp. 75–79.
[2] Andriacchi, T. P., 1993. Functional analysis of pre and post-knee surgery: total knee arthroplasty and ACL reconstruction. J. Biomech. Eng., **115**(4B), pp. 575–581.
[3] Lafortune, M. A., et al., 1992. Three-dimensional kinematics of the human knee during walking. J. Biomech., **25**(4), pp. 347–357.
[4] van Dijk, R., Huiskes, R., and Selvik, G., 1979. Roentgen stereophotogrammetric methods for the evaluation of the three dimensional kinematic behavior and cruciate ligament length patterns of the human knee joint. J. Biomech., **12**(9), pp. 727–731.
[5] Karrholm, J., et al., 1989. Chronic anterolateral instability of the knee. A roentgen stereophotogrammetric evaluation. Am. J. Sports Med., **17**(4), pp. 555–563.
[6] de Lange, A., Huiskes, R., and Kauer, J. M., 1990. Measurement errors in roentgen-stereophotogrammetric joint-motion analysis. J. Biomech., **23**(3), pp. 259–269.
[7] Selvik, G., 1989. Roentgen stereophotogrammetry. A method for the study of the kinematics of the skeletal system. Acta Orthop. Scand. Suppl., **232**, pp. 1–51.
[8] Andriacchi, T. P., et al., 1998. A point cluster method for in vivo motion analysis: applied to a study of knee kinematics. J. Biomech. Eng., **120**(6), pp. 743–749.
[9] Banks, S. A., and Hodge, W. A., 1996. Accurate measurement of three-dimensional knee replacement kinematics using single-plane fluoroscopy. IEEE Trans. Biomed. Eng., **43**(6), pp. 638–649.
[10] Stiehl, J. B., et al., 1995. Fluoroscopic analysis of kinematics after posterior-cruciate-retaining knee arthroplasty. J. Bone Joint Surg. Br., **77**(6), pp. 884–889.
[11] You, B. M., et al., 2001. In vivo measurement of 3-D skeletal kinematics from sequences of biplane radiographs: application to knee kinematics. IEEE Trans. Med. Imaging, **20**(6), pp. 514–525.

[12] Komistek, R. D., Dennis, D. A., and Mahfouz, M., 2003. In vivo fluoroscopic analysis of the normal human knee. Clin. Orthop., **(410)**, pp. 69–81.
[13] Li, G., et al., 1999. A validated three-dimensional computational model of a human knee joint. J. Biomech. Eng., **121**(6), pp. 657–662.
[14] Asano, T., et al., 2001. In vivo three-dimensional knee kinematics using a biplanar image-matching technique. Clin. Orthop., **(388)**, pp. 157–166.
[15] Li, G., et al., 2002. Biomechanics of posterior-substituting total knee arthroplasty: an in vitro study. Clin. Orthop., **(404)**, pp. 214–225.
[16] Dennis, D. A., et al., 1996. In vivo knee kinematics derived using an inverse perspective technique. Clin. Orthop., **(331)**, pp. 107–117.
[17] Freeman, M. A., and Pinskerova, V., 2003. The movement of the knee studied by magnetic resonance imaging. Clin. Orthop., **(410)**, pp. 35–43.